

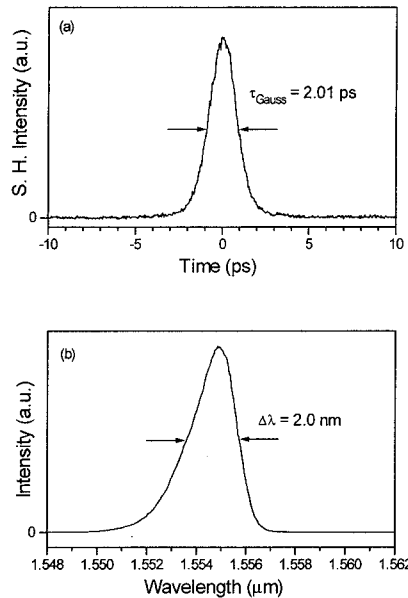
**CTuH5 Fig. 1** Laser cavity schematic. SLA: semiconductor laser amplifier, FI: Faraday isolator, PC: polarization controller.

monolithic semiconductor lasers with intra-cavity electroabsorption modulator (EAM) sections<sup>5</sup> and hybrid external-cavity semiconductor lasers. The nonlinear attenuation with applied voltage characteristic of EAMs results in short temporal transmission windows, making them attractive for modelocking applications, as the "effective" modulation frequency can be much higher than the applied electrical driving frequency. They tend, however, to be damaged by the high peak powers that can occur within erbium fiber lasers, particularly in the case of Q-switching. We report a novel 10-GHz actively modelocked unidirectional ring laser constructed from discrete components that uses a semiconductor laser amplifier as the gain medium and a short temporal switching window EAM as an amplitude modulator.

The laser cavity configuration is shown schematically in Fig. 1. It was composed entirely from fiber-pigtailed devices. Gain was provided by an InGaAsP semiconductor laser amplifier (SLA). Following the SLA a fixed 6-nm bandpass filter was included to constrain the lasing wavelength. A polarization controller (PC) was added to adjust the state of polarization injected to the EAM. The loop was completed with a fused fiber coupler, which provided a 10% output. The output pulses produced were measured using a scanning autocorrelator and optical spectrum analyzer, and in all cases the pulse shape was assumed to be Gaussian, as predicted by AM active modelocking theory.

The output pulses were found to be ~5 ps long with a time-bandwidth product of 0.73, indicating that they were significantly chirped. Previous studies have shown that EAMs can provide large degrees of approximately linear chirp and by splicing a length of dispersion compensating fiber to the output of the laser it was possible to compress these pulses down to 2.01 ps. The spectral FWHM was 2.0 nm, yielding a time-bandwidth product of 0.50, which indicates that these compressed pulses were close to transform-limited. Figures 2a and 2b show the autocorrelation trace and spectrum of these pulses, respectively.

The use of a tunable filter with a bandwidth of 2.65 nm resulted in the generation of slightly longer 3-ps pulses, but had the advantage that the central wavelength could be selected. Adjustment of this filter and the EAM driving frequency allowed tuning of the laser output. It was possible to produce pulses of <3.5 ps duration over a continuously tunable range from 1548–1565 nm. These lower and upper wave-



**CTuH5 Fig. 2** (a) Autocorrelation trace and (b) spectrum of the chirp-compensated 2-ps output pulses.

length limits were determined by the gain bandwidth of the SLA and the operating range of the EAM respectively. Despite the fact that no active stabilization techniques were employed and the entire cavity was composed of non-polarization-maintaining fiber the laser was found to be stable under laboratory conditions for timescales of an hour or more.

In summary, we report the generation of 2-ps transform-limited pulses at a repetition rate of 10 GHz, and 3-ps pulses tunable over a range of 17 nm from a novel actively modelocked semiconductor ring laser constructed from discrete fiber-pigtailed components. It is likely that even shorter pulses may be generated over a wider tuning range through optimization of the filter bandwidth and gain characteristics of the SLA.

\*BT Laboratories, Martlesham Heath, Ipswich, IP5 7RE, U.K.

1. Th. Pfeiffer, and G. Veith, *Electron. Lett.* **29**, 1849–1850 (1993).
2. M. Nakazawa, E. Yoshida, Y. Kimura, *Electron. Lett.* **30**, 1603–1605 (1994).
3. M. Nakazawa, E. Yoshida, K. Tamura, *Electron. Lett.* **32**, 1285–1287 (1996).
4. E. J. Greer, Y. Kimura, K. Suzuki, E. Yoshida, M. Nakazawa, *Electron. Lett.* **30**, 1764–1765 (1994).
5. K. Sato, I. Kotaka, Y. Kondo, M. Yamamoto, in *Optical Fiber Communication Conference*, Vol. 8, 1995 OSA Technical Digest Series (Optical Society of America, Washington, DC, 1995), pp 37–38.

CTuH6

11:45 am

### Time-resolved spectral analysis of phase conjugation by four-wave mixing in semiconductor optical amplifiers

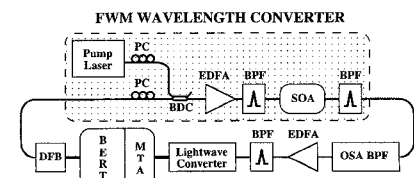
David F. Geraghty, Robert B. Lee, Kerry J. Vahala, Marc Verdiell,\* Mehrdad Ziari,\* Atul Mathur,\* *Department of Applied Physics, Mail Stop 128-95, California Institute of Technology, Pasadena, California 91125; E-mail: geraghty@cco.caltech.edu*

Optical phase conjugation provides a mechanism for achieving dispersion compensation in optical fibers.<sup>1</sup> This has been demonstrated by four-wave mixing (FWM) in both fiber<sup>2</sup> and semiconductor optical amplifiers (SOAs).<sup>3</sup> Imperfect phase conjugation will prevent exact reconstruction of a dispersed data stream. Here we use time-resolved spectral analysis (TRSA)<sup>4</sup> to evaluate the performance of FWM in SOAs for phase conjugation.

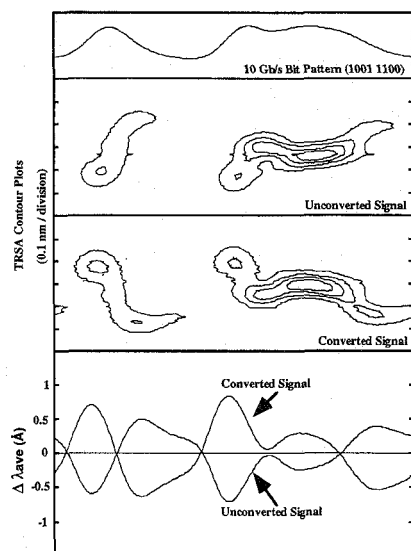
The system utilized is shown in Fig. 1. A bit-error-rate tester (BERT) generates 10 Gb/s data, which directly drives a distributed feedback laser. For time-resolved spectral analysis, the signal is put through a narrow bandpass filter (BPF), the OSA BPF, before detection. This BPF has a bandwidth of 0.08 nm and is stepped by 0.005 nm for the measurements. The filtered signal is then amplified in an erbium-doped fiber amplifier (EDFA) and passed through a 1-nm-wide BPF. This signal is detected with a lightwave converter, consisting of a PIN detector and a DC-coupled electrical preamplifier. The received signal is analyzed by a microwave transition analyzer (MTA), with a temporal resolution of about 3 ps.

Analysis is performed both on data converted by a FWM SOA wavelength converter, shown in Fig. 1, and on unconverted data. In the converter, the pump is a tunable, external-cavity diode laser. The pump and input signal each pass through a polarization controller (PC) before they are combined in a bidirectional coupler (BDC). The pump is adjusted for a 6-dB pump-to-signal ratio and a 6-nm shift. These signals are amplified in a high-power EDFA and passed through a 10-nm-wide BPF for ASE prefiltering before they are input into the SOA (a fiber pigtailed unit from SDL based on a multiple quantum-well compressively strained medium with 25-dB fiber-to-fiber gain). The SOA is followed by another BPF to isolate the converted signal.

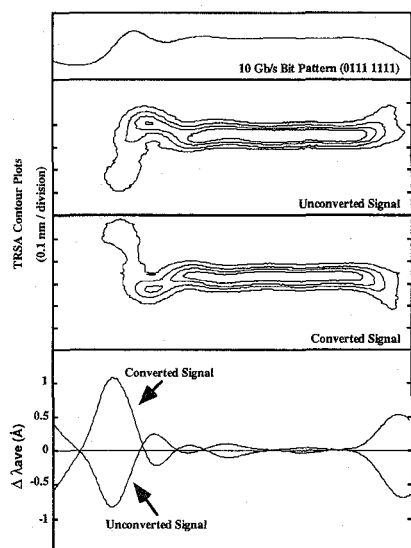
Due to the operating restrictions of our MTA, we are limited to data patterns that are eight bits in length. Results for two patterns are shown in Fig. 2. The linear scale TRSA contour plots of constant power have vertical and horizontal axes of time and frequency, respectively.



**CTuH6 Fig. 1** Experimental setup.



(a)



(b)

**CTuH6** Fig. 2 Results for pattern (a) 1001 1100 and (b) 0111 1111. The top panel shows the complete bit pattern. The middle two panels show linear-scale contours of constant powers for the unconverted and the converted signal. The bottom panel plots the average wavelength of both signals.

They clearly show the spectral inversion from the conversion. Another useful result is the average wavelength of the signal versus time.<sup>5</sup> For the patterns tested, the conversion increases the span of the average wavelength by as much as 0.05 nm. These results will be discussed in greater detail in terms of laser dynamics and phase conjugation in the talk.

We have utilized time-resolved spectral analysis to investigate the performance of FWM in SOAs as a phase conjugator. The spectral inversion is shown, however there is measurable signal alteration.

The authors wish to thank Al Benzoni for useful discussions.

\*SDL, San Jose, California 95134

1. D. M. Pepper, A. Yariv, *Opt. Lett.* **5**, 59–60 (1980).
2. S. Watanabe, T. Naito, T. Chikama, *IEEE Photon. Technol. Lett.* **5**, 92–95 (1993).
3. M. C. Tatham, X. Gu, L. D. Westbrook, G. Sherlock, D. M. Spirit, *Electron. Lett.* **30**, 1335–1336 (1994).
4. R. A. Linke, *IEEE J. Quantum Electron.* **QE-21**, 593–597 (1985).
5. T. L. Koch, R. A. Linke, *Appl. Phys. Lett.* **48**, 613–615 (1986).

## CTul

10:30 am–12:00 m

Rooms 316/317

### Nonlinear Applications for Sources

P. Likamwa, *University of Central Florida, CREOL, Presider*

## CTul1

10:30 am

### A solid-state, Nd:YAG laser-based source at 580 nm

H. M. Pask, J. A. Piper, *Centre for Lasers and Applications, Macquarie University, N.S.W., 2109, Australia; E-mail: hpask@macadam.mq.edu.au*

We report a simple scheme based on a combination of two nonlinear processes, stimulated Raman scattering (SRS) and second-harmonic generation (SHG), which converts the wavelength of Nd:YAG laser output at 1064–580 nm. This wavelength is close to the optimum wavelength for a range of laser-based dermatological procedures including the removal of vascular lesions. At present, laser sources used for these procedures include pulsed dye lasers (~585 nm), krypton ion lasers (565 nm) and copper vapor lasers (578 nm), and clearly a solid-state device generating in this spectral region would be an attractive alternative to the laser sources currently in use.

Solid-state Raman-active crystals are attractive media for SRS, offering high gain and better thermal characteristics than more widely used, gaseous media. Efficient SRS in  $\text{LiIO}_3$  crystals was first reported in 1975,<sup>1</sup> while frequency conversion of Nd:YALO laser output to various visible wavelengths through SRS and either SHG or sum frequency generation (SFG) using  $\text{LiIO}_3$  as both a Raman-active and frequency-mixing crystal has also been reported.<sup>2</sup> More recent progress in solid-state Raman lasers in other crystals is briefly reviewed in Ref. 3. The availability of new and high-quality crystal materials and the demand for compact visible laser sources has led us to re-examine SRS in crystals as an approach to developing new sources.

The initial pump source for our experiments is an arclamp-pumped Quantronix 114 Nd:YAG laser, which is typically AO Q-switched at repetition rates from 1–100 kHz and produces up to 5 W average power in a TEM<sub>00</sub> mode at high repetition rates. The resonator was modified to enable SRS and SHG to be investigated using intracavity configurations, as these were found to offer higher con-

version efficiencies and a lower incidence of crystal damage. This entailed lengthening the cavity to accommodate the nonlinear crystals, and the use of cavity mirrors that provided a high-Q resonator for the fundamental (1064 nm), various output couplings at the first Stokes wavelength (typically 10–50%), and high transmission at 580 nm.

Intracavity SRS has been investigated as a function of lamp current, pulse-repetition frequency and output coupling. The Raman shift and threshold depend on crystal length, cut and orientation relative to the pump polarization. For the results reported here, a 4-cm crystal was used, cut for propagation along the a-axis and oriented so that both the pump and Stokes waves propagated as o-waves. The Stokes output occurred at 1159 nm, corresponding to a Raman shift of 770  $\text{cm}^{-1}$ , and consistent with separate observations of the spontaneous Raman spectra obtained using a microRaman spectrometer. The threshold intracavity pump power for observing SRS was measured to be  $\sim 1 \text{ MW/cm}^2$ . Various aspects of the SRS process that have been investigated include the temporal evolution of the pump and Stokes pulses, beam quality issues and conversion efficiency. In excess of 1 W average power at 1159 nm was obtained for 20% output coupling and for repetition rates from 3–6 kHz.

Frequency doubling of the first Stokes output has been obtained using both intracavity and extracavity configurations, with the highest conversion efficiencies obtained by placing an AR-coated LBO crystal ( $3 \times 3 \times 5 \text{ mm}$ ) intracavity. The crystal was cut for type 1 phase-matching of 1064/532 nm, but could be rotated by  $11^\circ$  for phase-matching of 1179/580 nm. In order to maximize the output at 580 nm a three-mirror folded resonator was used, and a maximum output of 480 mW was obtained in a 3-kHz pulse train, with a conversion efficiency of 22% with respect to intracavity power at 1160 nm.

We are currently examining the prospects for scaling this device to higher average powers, and for demonstrating a diode-pumped device.

1. E. O. Amman and J. Falk, *Appl. Phys. Lett.* **22**, 662, (1975).
2. E. O. Amman, *J. Appl. Phys.* **51**, 118 (1980).
3. J. T. Murray, R. C. Powell, N. Peyghambarian, *J. Luminescence* **66 & 67**, 89, (1996).

## CTul2

10:45 am

### Generation of continuous wave radiation at 317 nm by frequency doubling of a diode laser

H. Talvitie, A. Seppänen, A. Äijälä, E. Ikonen, *Metrology Research Institute, Helsinki University of Technology, Otakaari 5A, FIN-02150 Espoo, Finland; E-mail: hannu.talvitie@hut.fi*

Compact, reliable, and cost-efficient ultraviolet (UV) laser sources are attractive for many applications including radiometric characterization of detectors in the biologically interest-